

ResCLIP: Residual Attention for Training-free Dense Vision-language Inference

Yuhang Yang* Jinhong Deng* Wen Li† Lixin Duan
 University of Electronic Science and Technology of China
 {yvhyang, jhdengvision, liwenbnu, lxduan}@gmail.com

Abstract

While vision-language models like CLIP have shown remarkable success in open-vocabulary tasks, their application is currently confined to image-level tasks, and they still struggle with dense predictions. Recent works often attribute such deficiency in dense predictions to the self-attention layers in the final block, and have achieved commendable results by modifying the original query-key attention to self-correlation attention, (e.g., query-query and key-key attention). However, these methods overlook the cross-correlation attention (query-key) properties, which capture the rich spatial correspondence. In this paper, we reveal that the cross-correlation of the self-attention in CLIP’s non-final layers also exhibits localization properties. Therefore, we propose the Residual Cross-correlation Self-attention (RCS) module, which leverages the cross-correlation self-attention from intermediate layers to remold the attention in the final block. The RCS module effectively reorganizes spatial information, unleashing the localization potential within CLIP for dense vision-language inference. Furthermore, to enhance the focus on regions of the same categories and local consistency, we propose the Semantic Feedback Refinement (SFR) module, which utilizes semantic segmentation maps to further adjust the attention scores. By integrating these two strategies, our method, termed **ResCLIP**, can be easily incorporated into existing approaches as a plug-and-play module, significantly boosting their performance in dense vision-language inference. Extensive experiments across multiple standard benchmarks demonstrate that our method surpasses state-of-the-art training-free methods, validating the effectiveness of the proposed approach. Code is available at <https://github.com/yvhyangyang/ResCLIP>.

1. Introduction

Recently, we have witnessed the unprecedented breakthrough of vision-language models (VLMs) [9, 14, 26, 37,

*Yuhang Yang and Jinhong Deng contributed equally.

†Corresponding author.

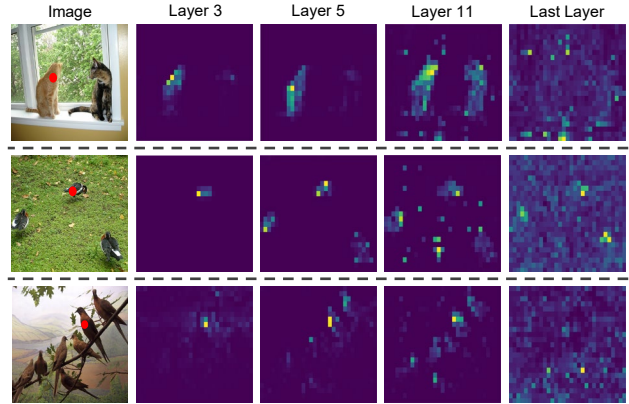


Figure 1. The attention visualization from different layers of CLIP [38] model. The images are sampled from PASCAL VOC [17] dataset.

[38], which are de facto foundation models across various downstream tasks such as zero-shot classification [21, 38], natural language processing [7, 15, 39] and visual question answering [3, 24, 56]. Especially, VLMs exhibit surprising open-vocabulary recognition capabilities because they are trained on large-scale image-text pairs with contrastive learning. Despite impressive performance achieved in image-level open-vocabulary tasks, they struggle with dense prediction tasks such as semantic segmentation due to the well-known limitation in localization ability [40, 46].

To this end, some previous works [10, 34, 41, 48, 50, 51, 58] make great efforts to address these limitations by fine-tuning CLIP with pixel-level annotations. These methods [34, 52, 62] not only consume expensive annotation costs but also are easily biased toward the training data, eliminating the generalization ability within CLIP. This has motivated a growing interest in training-free methods [19, 28, 29, 42, 46, 60] that aim to adapt pre-trained representations of CLIP for semantic segmentation without additional training and maximumly maintain the generalization ability of CLIP simultaneously. These approaches typically attribute the inferior results of CLIP on dense prediction to the self-attention layer in the last block of CLIP (last col. in Fig. 1), which presents spatial-invariant attention. For example, SCLIP proposes to replace orig-

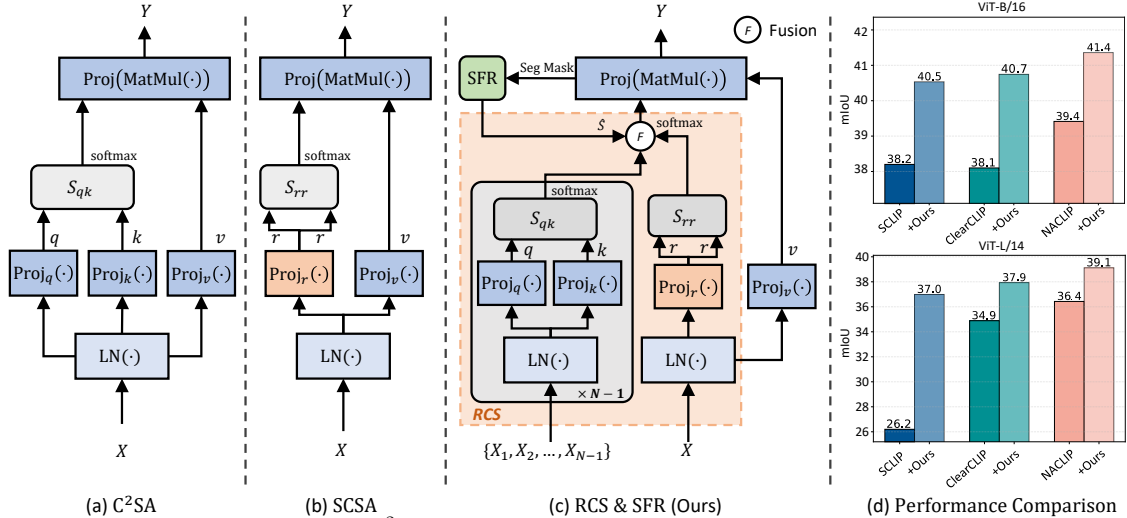


Figure 2. (a) Cross-correlation self-attention (C²SA). The query and key are mapped by different project matrices. The attention is obtained by matrix multiplication between query and key. (b) Self-correlation self-attention (SCSA). The attention is calculated by the self-correlation such as key-key or query-query. (c) Residual Cross-correlation Self-attention (RCS) and Semantic Feedback Refinement (SFR). (d) The performance comparison between our methods and baselines.

inal query-key self-attention with query-query and key-key self-attention. NACLIP [19] employs key-key self-attention with neighbor priors to enhance attention across adjacent patches. We summarize these attention paradigms as self-correlation self-attention (SCSA, Fig. 2(b)), which achieves better spatial-covariant features than the original last self-attention layer (Fig. 2(a)). However, they overlook the cross-correlation self-attention (C²SA)¹ properties that capture the diverse and spatial correspondence. Ideally, if the attention is supervised by the pixel-level data, the C²SA will learn densely class-specific representations. We, therefore, ask: *Can we obtain such properties of the C²SA from CLIP even if it does not receive pixel-level supervision?*

We answer this question by examining the C²SA in all layers and reveal that the attention of C²SA in non-last layers exhibits localization properties unlike that in the last layer. We visualize the attention of CLIP across different layers in Fig. 1. We can observe that the attention in the last layer is spatial-invariant while the attentions in other layers exhibit class-specific features and localization properties. For example, the attention of the “cat” in the top image can attend to other “cat” regions in the image to some extent. This motivates us to propose a novel Residual Cross-correlation Self-attention (RCS) that borrows the cross-correlation self-attention from intermediate layers to make a residual connection with the attention in the last block. The cross-correlation could reorganize the spatial information thus unleashing the potential of CLIP for dense vision-language inference. Moreover, to explicitly enhance

¹For clarity, cross-correlation self-attention (C²SA) is the standard self-attention that uses query and key to calculate attention. In contrast, self-correlation self-attention (SCSA) uses query or key pairs solely to calculate attention, such as key-key or query-query attention.

the focus on regions of the same categories and local consistency, we also propose a Semantic Feedback Refinement (SFR) module to leverage the semantic segmentation map to further tweak the attention score. It is worth noting that our method termed **ResCLIP** (Fig. 2(c)) is orthogonal to existing works and can be seamlessly integrated into existing approaches as a plug-and-play module.

We conduct extensive experiments across eight segmentation benchmarks, demonstrating CLIP’s substantial potential for open-vocabulary segmentation. As a plug-and-play solution, we integrate our method with three leading models: SCLIP, ClearCLIP, and NACLIP. The experimental results demonstrate significant improvements, with consistent mIoU gains across all datasets. As shown in Fig. 2(d), equipped with our method, the performance will be significantly boosted across all models. For example, our method makes improvements from 1.7% to 13.1% mIoU compared with counterparts. We also have conducted many ablation studies in both quantitative and qualitative ways to analyze the components of our method.

Our contributions can be summarized as follows:

- We reveal that attention from intermediate layers of CLIP exhibits class-specific features and localization properties. To the best of our knowledge, this work is the first work to discover that the cross-correlation self-attention from intermediate layers present localization properties and can heal the attention in the last layer.
- We propose a novel training-free approach, terms ResCLIP, including Residual Cross-correlation Self-attention (RCS) and Semantic Feedback Refinement (SFR) modules. These two modules can rectify the attention in the last layer to capture class-specific features and

local consistency so that improve CLIP model for dense vision-language prediction tasks.

- We have conducted extensive experiments on open-vocabulary semantic segmentation tasks including eight widely used benchmarks. The results in experiments demonstrate the effectiveness of our proposed method.

2. Related Work

Vision-language Foundation Models. In recent years, VLMs have emerged as a general paradigm in various vision tasks, demonstrating remarkable capabilities in zero-shot and few-shot learning scenarios. Unlike Segment Anything Model (SAM) [26, 54, 63] which focus on promoting semantic-agnostic segmentation, a series of contrastive learning-based approaches [1, 11, 21, 30, 35, 38, 49, 55, 57] have shown exceptional adaptability across diverse downstream tasks. CLIP, in particular, achieves robust vision-text alignment through training on image-text pairs [18, 47, 53]. This has spawned numerous extensions to expand tasks such as visual question answering [24, 25], image captioning [31] and downstream inference capabilities [11, 45].

Open-vocabulary Semantic Segmentation (OVSS). The OVSS extends traditional segmentation by enabling pixel-level dense prediction for arbitrary categories specified through text descriptions. Recent advances in vision-language models, particularly CLIP, have catalyzed significant progress [11, 38, 49] in this field. For their supervision requirements: fully-supervised methods [20, 22, 33] that fine-tune CLIP using pixel-level annotations, weakly-supervised approaches [10, 34, 41, 48, 48, 50, 51, 58] that leverage image-text pairs for training, and training-free methods [6, 19, 23, 28, 32, 38, 43, 46, 60] that modify CLIP’s architecture with minimal changes. While fully-supervised methods achieve strong performance but require extensive labeled data, and weakly-supervised methods like GroupViT [50] introduce specialized architectures with group tokens, training-free approaches such as MaskCLIP [60] focus on adapting CLIP’s self-attention mechanisms to enable dense prediction capabilities. However, these existing methods often struggle to fully utilize CLIP’s semantic understanding due to limited fine-tuning datasets [44] and their local understanding capability.

Different Self-attention for Dense Visual Features. Recent training-free approaches show great interest in modifying attention mechanisms to enhance CLIP’s dense visual representation capabilities. While vanilla CLIP employs query-key multiplication to obtain holistic visual representations that are invariant to spatial positions [61], subsequent works have explored various attention modifications. SCLIP[46] introduces self-correlation attention by combining query-query and key-key products as final layer attention weights to capture spatial-covariant features. This was followed by approaches such as GEM [6] presents

a way to calculate the attention matrix as the combination of query-query, query-key and value-value attention, NAACLIP [19] emphasizes key-key products with Gaussian kernels, ClearCLIP [28] utilizes query-query interactions, CLIPtrase [42] tries to use weighted average of self-correlation attention to cluster the "global" patch for segmentation and ProxyCLIP [29] exploring attention combination with vision foundation models such as SAM. Different from these works, we discover that the cross-correlation self-attention from intermediate layers present localization properties and can heal the attention in the last layer. Therefore, we propose a novel training-free approach, terms ResCLIP, including Residual Cross-correlation Self-attention (RCS) and Semantic Feedback Refinement (SFR) modules. These two modules can rectify the attention in the last layer to capture class-specific features and local consistency so that improve CLIP model for dense vision-language prediction tasks.

3. Methodology

In this section, we begin with an introduction to CLIP and its application to open-vocabulary semantic segmentation in a training-free paradigm in Sec. 3.1. Then, we describe the design of the proposed method including Residual Cross-correlation Self-attention (RCS) and Semantic Feedback Refinement (SFR) modules in Sec. 3.2.

3.1. Preliminary

Vision Encoder Architecture of CLIP. CLIP utilizes a Vision Transformer (ViT) [38] to encode images into a representation aligning with textual descriptions. In conventional ViT [2], an input image $H \times W \times 3$ is partitioned into a grid of non-overlapping patches of size $P \times P$. This results in $h = H/P$ rows, and $w = W/P$ columns of patches. Each patch is then being projected into a d dimensional space, which can be presented by vectorized feature $x_i \in \mathbb{R}^d$ with preserved spatial relationships through explicit positional embeddings. Therefore, the input at each layer can be formulated as a sequence of visual tokens $X = \{x_{\text{cls}}, x_1, \dots, x_{h \times w}\} \in \mathbb{R}^{(1+hw) \times d}$, where x_{cls} denotes the class token to capture global information. These visual tokens will feed into several multi-head self-attention layers to obtain the final token representations.

Self-attention Module. The core of the transformer encoder is the self-attention mechanism (see Fig. 2(a)), which enables the model to capture relationships between different patches. Note that we only consider the single-head self-attention for simplicity. The self-attention is given by:

$$q, k, v = \text{Proj}_{q,k,v}(\text{LN}(X)), \quad (1)$$

$$S_{qk} = qk^T / \sqrt{d_k}, \quad (2)$$

$$\text{Attn}(S_{qk}) = \text{softmax}(S_{qk}) = \text{softmax}(qk^T / \sqrt{d_k}), \quad (3)$$

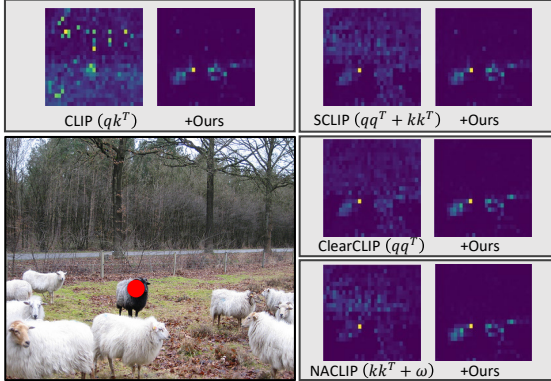


Figure 3. Comparison of attention maps across different versions of CLIP and ours.

where q, k, v indicates the query, key and value, respectively. The LN is layer normalization, Proj denotes a projection layer, and d_k is the dimension of key k . The attention scores $S_{qk} \in \mathbb{R}^{(1+hw) \times (1+hw)}$ imply the intrinsic global structural dependencies between patches, from which the attention map $\text{Attn}(S_{qk})$ is obtained through the softmax normalization.

Dense Vision-language Inference. CLIP was originally trained on large-scale image-text pairs using contrastive loss, demonstrating promising results in open-vocabulary image recognition tasks. The text representations $X_{\text{text}} = \{t_1, t_2, \dots, t_c\}$ are obtained through a text encoder and are used to align with cls token x_{cls} of visual features for each image-text pair. A natural idea is to extend the CLIP model to dense vision-language inference tasks such as open-vocabulary semantic segmentation by calculating the similarity between the dense visual tokens $X_{\text{dense}} = \{x_1, \dots, x_{h \times w}\} \in \mathbb{R}^{hw \times d}$ and text tokens X_{text} . In particular, we can obtain the segmentation map as follows,

$$\mathcal{M} = \arg \max \cos(X_{\text{dense}}, X_{\text{text}}). \quad (4)$$

However, the obtained semantic segmentation maps are full of noise due to the deficiency in localization ability in the CLIP model. The purpose of this work is to improve the performance of dense vision-language inference in a training-free manner so that maximumly reserves the generalization ability of CLIP by adjusting the attention in the last layers.

3.2. ResCLIP

As demonstrated in the previous works [60], CLIP exhibits inherent limitations in pixel-level semantic segmentation. To address these challenges, recent studies [19, 28, 46, 60] have proposed several approaches in a training-free manner and involve minimal modifications to the original model. These methods reveal that the attention in the last layer of CLIP exhibits spatial-invariant features, *i.e.*, local features tend to be invariant to their spatial position in the image.

Therefore, these methods [19, 28, 46] focus on reformulating the self-attention module in the final layer of CLIP by introducing a self-correlation self-attention (SCSA) to obtain the spatial-covariant features. These SCSA-based methods encourage each local token to attend to itself and the positions sharing similar features with it so that eliminates the spatial-invariant issues in the original CLIP, leading to improved dense prediction performance.

However, the SCSA enforces the self-similar features response and lacks the capacity to capture the cross-feature dynamics that cross-correlation self-attention (C^2SA) provides. The cross-correlation self-attention typically captures the diverse and spatial correspondence, which is beneficial for localization. But the C^2SA in the last layer has shown spatial-invariant properties in CLIP. Through careful experiments, we reveal that the self-attention in non-last layers of CLIP exhibits class-specific features and localization properties (See Fig. 1). For example, the attention of the “cat” in the top image can attend to other “cat” regions in the image to some extent.

Therefore, we propose a novel training-free approach that aggregates the C^2SA from intermediate layers of CLIP to remold the attention in the last block. The cross-correlation could reorganize the spatial information thus unleashing the potential of CLIP for dense vision-language inference. In particular, we propose a novel Residual Cross-correlation Self-attention (RCS) that aggregates the C^2SA from intermediate layers to make a residual connection with the attention in the last block. The RCS could reorganize the spatial information thus unleashing the potential of CLIP for dense vision-language inference. Moreover, to explicitly enhance the focus on regions of the same categories and local consistency, we also propose a Semantic Feedback Refinement (SFR) module to leverage the semantic segmentation map to further tweak the attention score. As shown in Fig. 3, our method could improve the attention of the baseline methods to attend more semantic-related regions. The overview of our method is present in Fig. 4.

3.2.1. Residual Cross-correlation Self-attention

The Residual Cross-correlation Self-attention (RCS) module borrows the attention from the intermediate layers to remold the attention module in the last layer. Specifically, we first extract the C^2SA from intermediate layers and aggregate information from them through the average operation. Formally, we denote the C^2SA attention $\text{Attn}^i(S_{qk})$ as \mathcal{A}_{qk}^i in i -th layer, the aggregated attention \mathcal{A}_c can be calculated as follows,

$$\mathcal{A}_c = \frac{1}{N} \sum_{i=s}^e \mathcal{A}_{qk}^i, \quad (5)$$

where $N = e - s + 1$ indicates the number of layers from the start layer s to the end layer e . Based on this aggregated

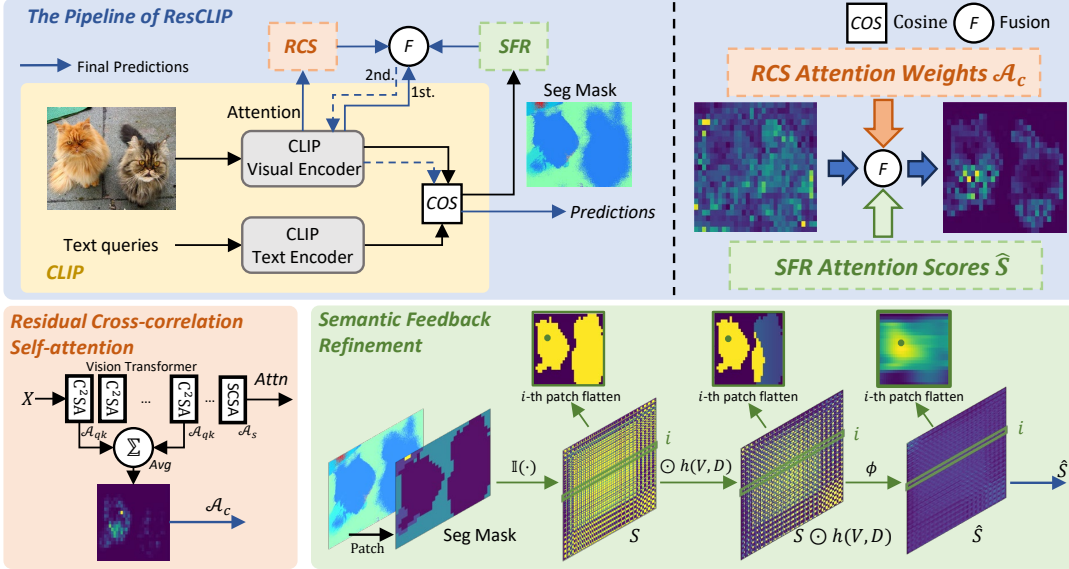


Figure 4. Overview of our ResCLIP consisting of Residual Cross-correlation Self-attention (RCS) and Semantic Feedback Refinement (SFR). The RCS module enhances CLIP’s attention mechanism by fusing C^2SA from non-last layers \mathcal{A}_c with SCSA \mathcal{A}_s to capture richer spatial information. The SFR module leverages an initial segmentation mask (black arrows) to refine attention scores. These refined attention scores \hat{S} are combined with RCS to adjust the attention in the last layer of CLIP and produce the final prediction (blue arrows).

attention, the RCS attention can be formulated as follows,

$$\mathcal{A}_{r_{cs}} = (1 - \lambda_{r_{cs}}) \cdot \mathcal{A}_s + \lambda_{r_{cs}} \cdot \mathcal{A}_c, \quad (6)$$

where \mathcal{A}_s is the SCSA attention used in previous works [28, 46] and $\lambda_{r_{cs}}$ is the trade-off parameter. Our RCS absorbs information from both the \mathcal{A}_s and \mathcal{A}_c , which capture the local patch structure and cross-feature correspondence. This attention could better reorganize the information in the last layer and improve the final classification.

3.2.2. Semantic Feedback Refinement

Although our RCS module not only provides spatial-invariant attention but also cross-feature dynamics, the attention is still not real attention under the pixel level supervision. Some works such as NAACLIP [19] add prior regularization to the attention by paying attention to the neighbor patches with discretized Gaussian kernels into attention maps. However, these kernels are isotropic and thus may introduce extra context due to the shapes of the objects being versatile. Besides, ideal attention should attend to the objects that share the same categories [37]. To this end, we propose a Semantic Feedback Refinement (SFR) module that improves the attention with the same semantics and maintains the locality simultaneously by using the semantic segmentation map from the CLIP model as feedback.

In particular, we begin with a semantic segmentation map, which is obtained by our RCS module, and then use this semantic segmentation map to further tweak the attention in the last layer. This loop would obtain better attention, resulting in improved performance. Formally, suppose

that we have an attention score $S \in \mathbb{R}^{hw \times hw}$, each element S_{ij} in S indicates the attention from i -th patch to j -th patch. Now, we consider there is a semantic segmentation map $\mathcal{M} \in \mathbb{R}^{hw}$. For brevity, we only consider the attention score $S^i \in \mathbb{R}^{hw}$ for one patch as an example, it can be obtained as follows,

$$S_{m,n}^i = \mathbb{I}(\mathcal{M}_{i',j'} == \mathcal{M}_{m,n}), \quad (7)$$

where $m \in \{1, 2, \dots, h\}$, $n \in \{1, 2, \dots, w\}$, $i' = \lfloor i/w \rfloor$ and $j' = (i \bmod w)$ indicates the grid index in mask \mathcal{M} for the i -row attention S^i . And the $\mathbb{I}(\cdot)$ is the indicator function where 1 when \cdot is true, otherwise 0.

To further maintain the locality, we emphasize the attention to the adjacent patches of the same class. We first identify connected and disjoint regions, then reduce the attention to the disjoint ones. To be specific, we first define a decay function as follows,

$$h(V, D) = V + (1 - V) \cdot D, \quad (8)$$

where V is the mask where $V_{mn} = 1$ if there a valid path from (m, n) to (i', j') , otherwise 0. D is a distance-based decay function, which is defined as:

$$D(p, q) = \exp\left(-\frac{d(p, q)}{\max(d(\cdot, \cdot))}\right), \quad (9)$$

where p and q denote the grid coordinates for the patches. We use the Chebyshev Distance for simplicity which measures the most significant difference with different patches as follows,

$$d(p, q) = \max(|p_x - q_x|, |p_y - q_y|). \quad (10)$$

Table 1. Open-vocabulary semantic segmentation quantitative comparison on datasets *without* a background class. Our results are marked in gray. The best results on each dataset for different encoders are **bolded**.

Methods	Training-free?	Encoder	VOC20	Context59	Stuff	Cityscape	ADE20k	Avg.
GroupViT [50]	×	ViT-S/16	79.7	23.4	15.3	11.1	9.2	27.7
CoCu [48]	×	ViT-S/16	-	-	13.6	15.0	11.1	-
TCL [10]	×	ViT-B/16	77.5	30.3	19.6	23.1	14.9	33.1
CLIP [38]	✓	ViT-B/16	41.8	9.2	4.4	5.5	2.1	12.6
MaskCLIP [60]	✓	ViT-B/16	74.9	26.4	16.4	12.6	9.8	28.0
ReCo [43]	✓	ViT-B/16	57.7	22.3	14.8	21.1	11.2	25.4
CLIPSurgery [32]	✓	ViT-B/16	-	-	21.9	31.4	-	-
SCLIP [46]	✓	ViT-B/16	80.4	34.2	22.4	32.2	16.1	37.1
+ResCLIP(ours)	✓	ViT-B/16	84.6	35.8	23.9	34.4	17.6	39.3 (+2.2)
ClearCLIP [28]	✓	ViT-B/16	80.9	35.9	23.9	30.0	16.7	37.5
+ResCLIP(ours)	✓	ViT-B/16	87.1	36.4	24.3	34.5	17.8	40.0 (+2.5)
NACLIP [19]	✓	ViT-B/16	79.7	35.2	23.3	35.5	17.4	38.2
+ResCLIP(ours)	✓	ViT-B/16	86.0	36.8	24.7	35.9	18.0	40.3 (+2.1)
CLIP [38]	✓	ViT-L/14	15.8	4.5	2.4	2.9	1.2	5.4
MaskCLIP [60]	✓	ViT-L/14	30.1	12.6	8.9	10.1	6.9	13.7
SCLIP [46]	✓	ViT-L/14	60.3	20.5	13.1	17.0	7.1	23.6
+ResCLIP(ours)	✓	ViT-L/14	83.9	30.6	21.2	32.2	15.8	36.7 (+13.1)
ClearCLIP [28]	✓	ViT-L/14	80.0	29.6	19.9	27.9	15.0	34.5
+ResCLIP(ours)	✓	ViT-L/14	84.2	33.4	22.3	34.1	17.9	38.4 (+3.9)
NACLIP [19]	✓	ViT-L/14	78.7	32.1	21.4	31.4	17.3	36.2
+ResCLIP(ours)	✓	ViT-L/14	85.5	34.5	23.4	33.7	18.2	39.1 (+2.9)

Therefore, we can apply the decay function to attention score S^i as follows,

$$\hat{S}^i = \phi(S^i \odot h(V, D)), \quad (11)$$

where ϕ is a conventional 1-dimensional Gaussian kernel to smooth the final attention score. This smoothing operation enhances the generalization of attention scores while preserving the row-independence property of the original attention mechanism. By employing the above operation to each row, we can obtain the entire attention score map \hat{S} . Finally, we combine the original attention scores with our semantic feedback refinement score, which can be formulated as follows,

$$S_r = (1 - \lambda_{sfr}) \cdot S_s + \lambda_{sfr} \cdot \hat{S}, \quad (12)$$

where S_s is the attention score of SCSA and λ_{sfr} is the trade-off parameter. Now, we lead to the final version of ResCLIP, the final attention can be given by:

$$\mathcal{A}_{ResCLIP} = (1 - \lambda_{rcs}) \cdot \mathcal{A}_{sfr} + \lambda_{rcs} \cdot \mathcal{A}_c, \quad (13)$$

where $\mathcal{A}_{sfr} = \text{softmax}(S_r)$. To this end, residual attention $\mathcal{A}_{ResCLIP}$ benefit from 1) SCSA attention that provides spatial-covariant features as mentioned in previous works [19, 46]; 2) C²SA attention from intermediate layers that capture the rich spatial correspondence; 3) SFR attention that explicitly enhances the focus on regions of the same categories and local consistency.

4. Experiments

4.1. Experimental Setups

Datasets. We conduct comprehensive evaluations on eight widely-adopted benchmark datasets for open-vocabulary semantic segmentation. Following prior works [19, 28, 46], these datasets can be categorized into two groups based on the presence of a background category, whose names are abbreviated in parentheses for brevity. Firstly, datasets with background category: PASCAL VOC 2012 [17] (VOC21), PASCAL Context [36] (Context60) and COCO Object [8] (Object). Secondly, datasets with background category: COCO-Stuff [8] (Stuff), Cityscapes [13] and ADE20K-150 [59]. Additionally, we follow the construction of removing the background class in PASCAL VOC20 [17] (VOC20) and PASCAL Context59 [36] (Context59). Specifically, input images are resized to have a shorter side of 336 pixels, except for Cityscapes, where we use 560 pixels due to its inherently high-resolution images. We perform slide inference using a 224×224 window with a stride of 112 following [5, 10, 19, 28, 32, 46, 50].

Baselines. We compare our work with a comprehensive range of OVSS methods, including direct baseline CLIP [38], previous state-of-the-art training-free approaches: MaskCLIP [60], ReCo [43], CLIPSurgery [32], GEM [6], SCLIP [46], NACLIP [19] and ClearCLIP [28]. We also include a few influential weakly supervised methods, such as GroupViT [50], CoCu [48], TCL [10], SegCLIP [34], OVSegmentor [51], PGSeg [58], and

Table 2. Open-vocabulary semantic segmentation quantitative comparison on datasets *with* a background class. Our results are marked in gray . The best results on each dataset for different encoders are **bolded**.

Methods	Training-free?	Encoder	VOC21	Context60	Object	Avg.
GroupViT [50]	×	ViT-S/16	50.4	18.7	27.5	32.2
SegCLIP [34]	×	ViT-S/16	52.6	24.7	26.5	34.6
OVSegmentor [51]	×	ViT-B/16	53.8	20.4	25.1	33.1
PGSeg [58]	×	ViT-S/16	53.2	23.8	28.7	35.2
ViewCo [41]	×	ViT-S/16	52.4	23.0	23.5	33.0
CoCu [48]	×	ViT-S/16	40.9	21.2	20.3	27.5
TCL [10]	×	ViT-B/16	51.2	24.3	30.4	35.3
CLIP [38]	✓	ViT-B/16	16.2	7.7	5.5	9.8
MaskCLIP [60]	✓	ViT-B/16	38.8	23.6	20.6	27.7
ReCo [43]	✓	ViT-B/16	25.1	19.9	15.7	20.2
CLIPSurgery [32]	✓	ViT-B/16	-	29.3	-	-
GEM [6]	✓	ViT-B/16	46.2	32.6	-	-
SCLIP [46]	✓	ViT-B/16	59.1	30.4	30.5	40.0
+ResCLIP(ours)	✓	ViT-B/16	60.7	32.9	34.3	42.7 (+2.7)
ClearCLIP [28]	✓	ViT-B/16	51.8	32.6	33.0	39.1
+ResCLIP(ours)	✓	ViT-B/16	59.0	32.9	34.0	42.0 (+2.9)
NACLIP [19]	✓	ViT-B/16	58.9	32.2	33.2	41.4
+ResCLIP(ours)	✓	ViT-B/16	61.1	33.5	35.0	43.2 (+1.8)
SCLIP [46]	✓	ViT-L/14	44.4	22.3	24.9	30.5
+ResCLIP(ours)	✓	ViT-L/14	52.8	28.7	30.9	37.4 (+6.9)
ClearCLIP [28]	✓	ViT-L/14	48.7	28.3	29.7	35.5
+ResCLIP(ours)	✓	ViT-L/14	50.7	29.8	31.1	37.2 (+1.7)
NACLIP [19]	✓	ViT-L/14	52.2	28.7	29.9	36.9
+ResCLIP(ours)	✓	ViT-L/14	54.1	30.9	32.5	39.2 (+2.3)

ViewCo [41]. Unless explicitly mentioned, all reported results are from the respective papers. Besides, we select recent state-of-the-art methods SCLIP [46], NACLIP [19], ClearCLIP [28] with specialized attention designs as baselines and evaluate our method’s performance when integrated with these approaches. We also present results based on the ViT-L/14 architecture for a comprehensive evaluation.

Implementation details. In our experiments, we utilize the implementations provided by MMSegmentation [12]. Following TCL [10], we abstain from computationally intensive post-processing techniques that could lead to unfair comparisons, such as PAMR [4] (used in TCL [10], NACLIP [19]) and DenseCRF [27] (used in ReCo [43]). We employ only standard ImageNet prompts [38] without additional textual prompting strategies. By default, our comparative experiments are conducted using the ViT-B/16 [16] backbone, with ablation studies and sensitivity analyses performed on top of NACLIP. Our approach operates in a fully training-free manner, requiring neither retraining nor fine-tuning. We evaluate all semantic segmentation tasks using the mean Intersection over Union (mIoU) metric.

4.2. Main Results

Quantitative results. Table. 1 summarizes the performance of various open-vocabulary semantic segmentation models on datasets without a background class. Our ResCLIP demonstrates significant improvements when integrated

with state-of-the-art approaches including SCLIP [46], ClearCLIP [28], and NACLIP [19]. Notably, when combined with NACLIP [19], our method achieves state-of-the-art performance, surpassing mainstream weakly supervised approaches. As a plug-and-play solution, consistent improvements are observed across all five datasets compared to the baseline methods, showing the great potential of ResCLIP. We also evaluate performance on ViT-L/14 and observe that when adapting to different backbones, existing methods typically decrease by over 2% mIoU, *e.g.*, SCLIP [46] has a particularly severe drop of 13.5% mIoU. However, with the integration of our method, this performance degradation is significantly mitigated, demonstrating the effectiveness of the proposed method. Additionally, we conduct the experiments on datasets with a background class. The results are present in Table. 2. We can observe that ResCLIP shows consistent improvements across all datasets with a background class over all the counterparts. Specifically, our method surpasses weakly supervised approaches such as GroupViT [50], achieving state-of-the-art performance of 43.2% mIoU when integrated with NACLIP [19] on the ViT-B/16 backbone. Regarding the results of the ViT-L/14, our method still provides substantial improvements compared with other baseline methods. These results validate that the method effectively reduces the noise of original attention in the last layer of CLIP.

Qualitative results. In Fig. 5, we present qualitative comparison results with training-free methods such as

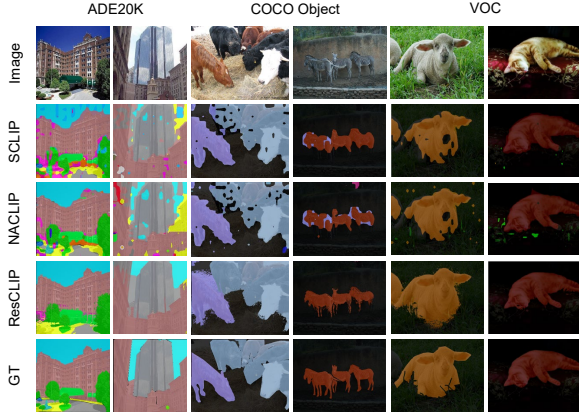


Figure 5. Qualitative comparison between different CLIP-based training-free segmentation methods.

Table 3. Ablation studies for the proposed method.

Methods	Module		mIoU	Δ
	RCS	SFR		
Baseline (NACLIP [19])	-	-	79.7	-
ResCLIP(Ours)	✓		85.5	+5.8
		✓	81.5	+1.8
	✓	✓	86.0	+6.3

SCLIP [46], NACLIP [19], and ClearCLIP [28]. From Fig. 5, our ResCLIP predicts higher quality and more accurate segmentation maps with reduced noise. ResCLIP demonstrates superior attention to the internal regions of an object, avoiding hollow dense predictions in central areas (e.g., the 1st col. in VOC and the 1st col. in COCO Object). Compared to NACLIP, which employs key-key attention in the last layer, ResCLIP achieves both effective noise reduction and clearer segmentation maps (e.g., on ADE20k), demonstrating that ResCLIP effectively captures rich spatial correspondences between objects of the same category, while SFR successfully enhances local consistency. More qualitative results can be referred to our Supplementary.

4.3. Experimental Analysis

Ablation studies. We conduct ablation studies using NA-CLIP with ViT-B/16 backbone, as shown in Table. 3. The RCS module alone improves mIoU from 79.7% to 85.5% on VOC20, demonstrating the effectiveness of incorporating non-last layers \mathcal{A}_{qk} information into the final attention map. The SFR module independently achieves a 1.8% mIoU improvement, validating its effectiveness in enhancing attention between semantically similar regions while preserving local spatial consistency. When combined, these modules achieve a substantial 6.3% mIoU improvement, reaching a mIoU of 86.0%, demonstrating their complementary utility.

Sensitivity analysis of hyper-parameters. In Fig. 6,

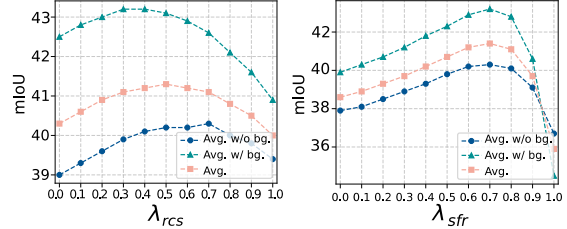


Figure 6. Analysis of hyper-parameters λ_{RCS} and λ_{SFR} .

Table 4. Analysis of layer fusion strategies in our method.

Fusion Ways		VOC20	Object
Methods	Layers		
<i>Cumulative Layers Aggregation</i>	1 \rightarrow 1	81.1	34.0
	1 \rightarrow 3	82.6	34.8
	1 \rightarrow 5	84.1	34.8
	1 \rightarrow 7	84.8	34.9
	1 \rightarrow 9	85.5	35.0
<i>Sliding Window Aggregation</i>	2 \rightarrow 5	84.2	34.8
	4 \rightarrow 7	85.0	34.7
	6 \rightarrow 9	86.0	35.0
	8 \rightarrow 11	85.8	34.8

we analyze the sensitivity of two key trade-off hyper-parameters λ_{RCS} and λ_{SFR} .

For λ_{RCS} , optimal performance is achieved when $\lambda_{RCS} = 0.5$. The parameter λ_{SFR} demonstrates best results at 0.7, with stable performance in the range of from 0.6 to 0.8. Both parameters exhibit similar trends: moderate values enhance performance while extreme values (e.g., 1.0) lead to degradation. This consistent behavior across different datasets suggests our method’s robustness, requiring only coarse hyper-parameter tuning for effective deployment.

Analysis of layer fusion strategies in RCS. As Eq. (5) shows, our RCS method averages attention from some layers. We explore two strategies for the aggregation (\mathcal{A}_{qk}) from non-last layers to capture the rich spatial correspondence. In Table. 4, we compare aggregation methods: Cumulative Layers Aggregation (CLA) and Sliding Window Aggregation (SWA). CLA starts from the first layer to the n -th while SWA applies a sliding window to aggregate attention where the window size is set to 4. From Table 4, we can observe that 1) for the CLA, the model increases the performance with more layers involved. 2) when leveraging the sliding window, the 6 \rightarrow 9 achieves the best results.

5. Conclusion

In this paper, we introduce ResCLIP, a novel framework that enhances CLIP’s ability for dense vision-language inference in a training-free manner. We discovered that attention from intermediate layers of CLIP exhibits class-specific features and localization properties. We propose two modules: Residual Cross-correlation Self-attention (RCS) and Semantic Feedback Refinement (SFR). These two modules not only provide rich spatial correspondence but also en-

hance the focus on the regions with the same semantics and local consistency to remold the attention in the last layer of CLIP. Extensive experiments show that ResCLIP improves performance across various benchmarks, demonstrating the effectiveness of the proposed method.

References

- [1] Jean-Baptiste Alayrac, Adria Recasens, Rosalia Schneider, Relja Arandjelović, Jason Ramapuram, Jeffrey De Fauw, Lucas Smaira, Sander Dieleman, and Andrew Zisserman. Self-supervised multimodal versatile networks. *NeurIPS*, 33:25–37, 2020. 3
- [2] Dosovitskiy Alexey. An image is worth 16x16 words: Transformers for image recognition at scale. *arXiv preprint arXiv:2010.11929*, 2020. 3
- [3] Stanislaw Antol, Aishwarya Agrawal, Jiasen Lu, Margaret Mitchell, Dhruv Batra, C Lawrence Zitnick, and Devi Parikh. Vqa: Visual question answering. In *ICCV*, pages 2425–2433, 2015. 1
- [4] Nikita Araslanov and Stefan Roth. Single-stage semantic segmentation from image labels. In *CVPR*, pages 4253–4262, 2020. 7
- [5] Luca Barsellotti, Roberto Amoroso, Lorenzo Baraldi, and Rita Cucchiara. Fossil: Free open-vocabulary semantic segmentation through synthetic references retrieval. In *WACV*, pages 1464–1473, 2024. 6
- [6] Walid Boussefham, Felix Petersen, Vittorio Ferrari, and Hilde Kuehne. Grounding everything: Emerging localization properties in vision-language transformers. In *CVPR*, pages 3828–3837, 2024. 3, 6, 7
- [7] Tom B Brown. Language models are few-shot learners. *arXiv preprint arXiv:2005.14165*, 2020. 1
- [8] Holger Caesar, Jasper Uijlings, and Vittorio Ferrari. Cocomp: Thing and stuff classes in context. In *CVPR*, pages 1209–1218, 2018. 6, 14, 16
- [9] Mathilde Caron, Hugo Touvron, Ishan Misra, Hervé Jégou, Julien Mairal, Piotr Bojanowski, and Armand Joulin. Emerging properties in self-supervised vision transformers. In *ICCV*, pages 9650–9660, 2021. 1
- [10] Junbum Cha, Jonghwan Mun, and Byungseok Roh. Learning to generate text-grounded mask for open-world semantic segmentation from only image-text pairs. In *CVPR*, pages 11165–11174, 2023. 1, 3, 6, 7
- [11] Mehdi Cherti, Romain Beaumont, Ross Wightman, Mitchell Wortsman, Gabriel Ilharco, Cade Gordon, Christoph Schuhmann, Ludwig Schmidt, and Jenia Jitsev. Reproducible scaling laws for contrastive language-image learning. In *CVPR*, pages 2818–2829, 2023. 3, 12, 14
- [12] MMSegmentation Contributors. Mmsegmentation: Openmmlab semantic segmentation toolbox and benchmark, 2020. 7
- [13] Marius Cordts, Mohamed Omran, Sebastian Ramos, Timo Rehfeld, Markus Enzweiler, Rodrigo Benenson, Uwe Franke, Stefan Roth, and Bernt Schiele. The cityscapes dataset for semantic urban scene understanding. In *CVPR*, pages 3213–3223, 2016. 6
- [14] Timothée Darcet, Maxime Oquab, Julien Mairal, and Piotr Bojanowski. Vision transformers need registers. *arXiv preprint arXiv:2309.16588*, 2023. 1
- [15] Jacob Devlin. Bert: Pre-training of deep bidirectional transformers for language understanding. *arXiv preprint arXiv:1810.04805*, 2018. 1
- [16] Alexey Dosovitskiy. An image is worth 16x16 words: Transformers for image recognition at scale. *arXiv preprint arXiv:2010.11929*, 2020. 7
- [17] Mark Everingham, SM Ali Eslami, Luc Van Gool, Christopher KI Williams, John Winn, and Andrew Zisserman. The pascal visual object classes challenge: A retrospective. *IJCV*, 111:98–136, 2015. 1, 6, 14, 17
- [18] Enrico Fini, Pietro Astolfi, Adriana Romero-Soriano, Jakob Verbeek, and Michal Drozdal. Improved baselines for vision-language pre-training. *arXiv preprint arXiv:2305.08675*, 2023. 3
- [19] Sina Hajimiri, Ismail Ben Ayed, and Jose Dolz. Pay attention to your neighbours: Training-free open-vocabulary semantic segmentation. In *WACV*, 2025. 1, 2, 3, 4, 5, 6, 7, 8, 12, 13, 14
- [20] Cong Han, Yujie Zhong, Dengjie Li, Kai Han, and Lin Ma. Open-vocabulary semantic segmentation with decoupled one-pass network. In *ICCV*, pages 1086–1096, 2023. 3
- [21] Chao Jia, Yinfei Yang, Ye Xia, Yi-Ting Chen, Zarana Parekh, Hieu Pham, Quoc Le, Yun-Hsuan Sung, Zhen Li, and Tom Duerig. Scaling up visual and vision-language representation learning with noisy text supervision. In *ICML*, pages 4904–4916. PMLR, 2021. 1, 3
- [22] Siyu Jiao, Yunchao Wei, Yaowei Wang, Yao Zhao, and Humphrey Shi. Learning mask-aware clip representations for zero-shot segmentation. *NeurIPS*, 36:35631–35653, 2023. 3
- [23] Dahyun Kang and Minsu Cho. In defense of lazy visual grounding for open-vocabulary semantic segmentation. *arXiv preprint arXiv:2408.04961*, 2024. 3
- [24] Aisha Urooj Khan, Hilde Kuehne, Chuang Gan, Niels Da Victoria Lobo, and Mubarak Shah. Weakly supervised grounding for vqa in vision-language transformers. In *ECCV*, pages 652–670. Springer, 2022. 1, 3
- [25] Wonjae Kim, Bokyung Son, and Ildoo Kim. Vilt: Vision-and-language transformer without convolution or region supervision. In *ICML*, pages 5583–5594. PMLR, 2021. 3
- [26] Alexander Kirillov, Eric Mintun, Nikhila Ravi, Hanzi Mao, Chloe Rolland, Laura Gustafson, Tete Xiao, Spencer Whitehead, Alexander C Berg, Wan-Yen Lo, et al. Segment anything. In *ICCV*, pages 4015–4026, 2023. 1, 3
- [27] Philipp Krähenbühl and Vladlen Koltun. Efficient inference in fully connected crfs with gaussian edge potentials. *NeurIPS*, 24, 2011. 7
- [28] Mengcheng Lan, Chaofeng Chen, Yiping Ke, Xinjiang Wang, Litong Feng, and Wayne Zhang. Clearclip: Decomposing clip representations for dense vision-language inference. In *ECCV*, 2024. 1, 3, 4, 5, 6, 7, 8, 12, 13, 14
- [29] Mengcheng Lan, Chaofeng Chen, Yiping Ke, Xinjiang Wang, Litong Feng, and Wayne Zhang. Proxyclick: Proxy

- attention improves clip for open-vocabulary segmentation. *arXiv preprint arXiv:2408.04883*, 2024. 1, 3
- [30] Junnan Li, Ramprasaath Selvaraju, Akhilesh Gotmare, Shafiq Joty, Caiming Xiong, and Steven Chu Hong Hoi. Align before fuse: Vision and language representation learning with momentum distillation. *NeurIPS*, 34:9694–9705, 2021. 3
- [31] Junnan Li, Dongxu Li, Caiming Xiong, and Steven Hoi. Blip: Bootstrapping language-image pre-training for unified vision-language understanding and generation. In *ICML*, pages 12888–12900. PMLR, 2022. 3
- [32] Yi Li, Hualiang Wang, Yiqun Duan, and Xiaomeng Li. Clip surgery for better explainability with enhancement in open-vocabulary tasks. *arXiv preprint arXiv:2304.05653*, 2023. 3, 6, 7
- [33] Feng Liang, Bichen Wu, Xiaoliang Dai, Kunpeng Li, Yinan Zhao, Hang Zhang, Peizhao Zhang, Peter Vajda, and Diana Marculescu. Open-vocabulary semantic segmentation with mask-adapted clip. In *CVPR*, pages 7061–7070, 2023. 3
- [34] Huaishao Luo, Junwei Bao, Youzheng Wu, Xiaodong He, and Tianrui Li. Segclip: Patch aggregation with learnable centers for open-vocabulary semantic segmentation. In *ICML*, pages 23033–23044. PMLR, 2023. 1, 3, 6, 7
- [35] Antoine Miech, Jean-Baptiste Alayrac, Lucas Smaira, Ivan Laptev, Josef Sivic, and Andrew Zisserman. End-to-end learning of visual representations from uncurated instructional videos. In *CVPR*, pages 9879–9889, 2020. 3
- [36] Roozbeh Mottaghi, Xianjie Chen, Xiaobai Liu, Nam-Gyu Cho, Seong-Whan Lee, Sanja Fidler, Raquel Urtasun, and Alan Yuille. The role of context for object detection and semantic segmentation in the wild. In *CVPR*, pages 891–898, 2014. 6
- [37] Maxime Oquab, Timothée Darcet, Théo Moutakanni, Huy Vo, Marc Szafraniec, Vasil Khalidov, Pierre Fernandez, Daniel Haziza, Francisco Massa, Alaaeldin El-Nouby, et al. Dinov2: Learning robust visual features without supervision. *arXiv preprint arXiv:2304.07193*, 2023. 1, 5
- [38] Alec Radford, Jong Wook Kim, Chris Hallacy, Aditya Ramesh, Gabriel Goh, Sandhini Agarwal, Girish Sastry, Amanda Askell, Pamela Mishkin, Jack Clark, et al. Learning transferable visual models from natural language supervision. In *ICML*, pages 8748–8763. PMLR, 2021. 1, 3, 6, 7, 13
- [39] Colin Raffel, Noam Shazeer, Adam Roberts, Katherine Lee, Sharan Narang, Michael Matena, Yanqi Zhou, Wei Li, and Peter J Liu. Exploring the limits of transfer learning with a unified text-to-text transformer. *JMLR*, 21(140):1–67, 2020. 1
- [40] Yongming Rao, Wenliang Zhao, Guangyi Chen, Yansong Tang, Zheng Zhu, Guan Huang, Jie Zhou, and Jiwen Lu. Denseclip: Language-guided dense prediction with context-aware prompting. In *CVPR*, pages 18082–18091, 2022. 1
- [41] Pengzhen Ren, Changlin Li, Hang Xu, Yi Zhu, Guanrun Wang, Jianzhuang Liu, Xiaojun Chang, and Xiaodan Liang. Viewco: Discovering text-supervised segmentation masks via multi-view semantic consistency. *arXiv preprint arXiv:2302.10307*, 2023. 1, 3, 7
- [42] Tong Shao, Zhuotao Tian, Hang Zhao, and Jingyong Su. Explore the potential of clip for training-free open vocabulary semantic segmentation. In *ECCV*, pages 139–156. Springer, 2025. 1, 3
- [43] Gyungin Shin, Weidi Xie, and Samuel Albanie. Reco: Retrieve and co-segment for zero-shot transfer. *NeurIPS*, 35: 33754–33767, 2022. 3, 6, 7
- [44] Shuyang Sun, Runjia Li, Philip Torr, Xiuye Gu, and Siyang Li. Clip as rnn: Segment countless visual concepts without training endeavor. In *CVPR*, pages 13171–13182, 2024. 3
- [45] Feng Wang, Manling Li, Xudong Lin, Hairong Lv, Alexander G Schwing, and Heng Ji. Learning to decompose visual features with latent textual prompts. *arXiv preprint arXiv:2210.04287*, 2022. 3
- [46] Feng Wang, Jieru Mei, and Alan Yuille. Sclip: Rethinking self-attention for dense vision-language inference. In *ECCV*, pages 315–332. Springer, 2025. 1, 3, 4, 5, 6, 7, 8, 12, 13, 14
- [47] Chaoyi Wu, Xiaoman Zhang, Ya Zhang, Yanfeng Wang, and Weidi Xie. Medclip: Medical knowledge enhanced language-image pre-training for x-ray diagnosis. In *ICCV*, pages 21372–21383, 2023. 3
- [48] Yun Xing, Jian Kang, Aoran Xiao, Jiahao Nie, Ling Shao, and Shijian Lu. Rewrite caption semantics: Bridging semantic gaps for language-supervised semantic segmentation. *NeurIPS*, 36, 2024. 1, 3, 6, 7
- [49] Hu Xu, Saining Xie, Xiaoqing Ellen Tan, Po-Yao Huang, Russell Howes, Vasu Sharma, Shang-Wen Li, Gargi Ghosh, Luke Zettlemoyer, and Christoph Feichtenhofer. Demystifying clip data. *arXiv preprint arXiv:2309.16671*, 2023. 3
- [50] Jiarui Xu, Shalini De Mello, Sifei Liu, Wonmin Byeon, Thomas Breuel, Jan Kautz, and Xiaolong Wang. Groupvit: Semantic segmentation emerges from text supervision. In *CVPR*, pages 18134–18144, 2022. 1, 3, 6, 7
- [51] Jilan Xu, Junlin Hou, Yuejie Zhang, Rui Feng, Yi Wang, Yu Qiao, and Weidi Xie. Learning open-vocabulary semantic segmentation models from natural language supervision. In *CVPR*, pages 2935–2944, 2023. 1, 3, 6, 7
- [52] Mengde Xu, Zheng Zhang, Fangyun Wei, Han Hu, and Xiang Bai. Side adapter network for open-vocabulary semantic segmentation. In *CVPR*, pages 2945–2954, 2023. 1
- [53] Jianwei Yang, Chunyuan Li, Pengchuan Zhang, Bin Xiao, Ce Liu, Lu Yuan, and Jianfeng Gao. Unified contrastive learning in image-text-label space. In *CVPR*, pages 19163–19173, 2022. 3
- [54] Xiaobo Yang and Xiaojin Gong. Tuning-free universally-supervised semantic segmentation. *arXiv preprint arXiv:2405.14294*, 2024. 3
- [55] Lewei Yao, Runhui Huang, Lu Hou, Guansong Lu, Minzhe Niu, Hang Xu, Xiaodan Liang, Zhenguo Li, Xin Jiang, and Chunjing Xu. Filip: Fine-grained interactive language-image pre-training. *arXiv preprint arXiv:2111.07783*, 2021. 3
- [56] Jiahui Yu, Zirui Wang, Vijay Vasudevan, Legg Yeung, Mojtaba Seyedhosseini, and Yonghui Wu. Coca: Contrastive captioners are image-text foundation models. *arXiv preprint arXiv:2205.01917*, 2022. 1
- [57] Lu Yuan, Dongdong Chen, Yi-Ling Chen, Noel Codella, Xiyang Dai, Jianfeng Gao, Houdong Hu, Xuedong Huang,

- Boxin Li, Chunyuan Li, et al. Florence: A new foundation model for computer vision. *arXiv preprint arXiv:2111.11432*, 2021. 3
- [58] Fei Zhang, Tianfei Zhou, Boyang Li, Hao He, Chaofan Ma, Tianjiao Zhang, Jiangchao Yao, Ya Zhang, and Yanfeng Wang. Uncovering prototypical knowledge for weakly open-vocabulary semantic segmentation. *NeurIPS*, 36:73652–73665, 2023. 1, 3, 6, 7
- [59] Bolei Zhou, Hang Zhao, Xavier Puig, Tete Xiao, Sanja Fidler, Adela Barriuso, and Antonio Torralba. Semantic understanding of scenes through the ade20k dataset. *IJCV*, 127:302–321, 2019. 6, 14, 15
- [60] Chong Zhou, Chen Change Loy, and Bo Dai. Extract free dense labels from clip. In *ECCV*, pages 696–712. Springer, 2022. 1, 3, 4, 6, 7
- [61] Tianfei Zhou, Fei Zhang, Boyu Chang, Wenguan Wang, Ye Yuan, Ender Konukoglu, and Daniel Cremers. Image segmentation in foundation model era: A survey. *arXiv preprint arXiv:2408.12957*, 2024. 3
- [62] Ziqin Zhou, Yinjie Lei, Bowen Zhang, Lingqiao Liu, and Yifan Liu. Zegclip: Towards adapting clip for zero-shot semantic segmentation. In *CVPR*, pages 11175–11185, 2023. 1
- [63] Xueyan Zou, Jianwei Yang, Hao Zhang, Feng Li, Linjie Li, Jianfeng Wang, Lijuan Wang, Jianfeng Gao, and Yong Jae Lee. Segment everything everywhere all at once. *NeurIPS*, 36, 2024. 3

ResCLIP: Residual Attention for Training-free Dense Vision-language Inference

Supplementary Material

In this supplementary document, we present additional materials not included in the main manuscript due to page limitations. The supplementary content is outlined:

- Sec. A: Additional attention comparison between the proposed method and previous works.
- Sec. B: Ablation studies on different ViT backbones.
- Sec. C: Extension on other CLIP-like models.
- Sec. D: More segmentation visualization results.

Now, we will present these materials as follows.

A. Attention Comparison

To further illustrate the impact of ResCLIP on attention mechanisms beyond examples shown in Fig. 3 in main paper, we present additional attention visualizations in Fig. A1. These visualizations demonstrate how our method enhances the attention maps across different training-free open-vocabulary semantic segmentation (OVSS) models so that our method could better aggregate information from previous layers. From Fig. A1, we can observe that our ResCLIP could attend to regions sharing similar class-specific features while previous works usually exhibit spatial-invariant features or focus on the local patches.

In particular, after integrating our Residual Cross-correlation Self-attention (RCS) and Semantic Feedback Refinement (SFR) modules into existing works, the attention maps show two key improvements: 1) enhanced local patches awareness and 2) strengthened global semantic correspondence. For example, in the left part of Fig. A1, we observe that previous works fail to effectively capture features from other “sheep” instances while our method can not only capture information from semantically consistent objects but also maintain local consistency. Similar phenomena can be observed from the right example in Fig. A1. Moreover, we can see that intermediate layers (*e.g.*, layers 5 and 11) show decent class-specific feature correspondence ability, which motivates us to incorporate them to remold the attention in the last block of CLIP.

B. Ablation Studies on ViT Backbones

In the main manuscript, we demonstrate effectiveness of the proposed RCS and SFR modules on ViT-B/16 backbone. To further demonstrate their generalization on other ViT backbones, we conduct additional experiments of ablation studies across ViT-B/16, ViT-B/32, and ViT-L/14 backbones. Moreover, we also evaluate our ResCLIP method by integrating it with previous training-free counterparts, *i.e.*, SCLIP [46], ClearCLIP [28], and NACLIP [19].

The experimental results are shown in Table. A1. We

can see that both RCS and SFR modules contribute substantially to performance improvements across multiple backbones and baselines, demonstrating the great generalization of our proposed modules. Specifically, taking NACLIP with ViT-B/16 as an example, Our RCS improves the average mIoU from 39.4% to 40.6%, while SFR increases it to 40.7%. When combining both modules, the performance further improves to 41.4%, suggesting complementary benefits from both components. Similar patterns are observed with other baseline methods.

Notably, our method demonstrates robust performance across different backbone architectures. For instance, when applied to SCLIP with ViT-L/14, ResCLIP significantly improves the average performance from 26.2% to 37.0%, showing particular effectiveness on larger architectures. The improvement is consistent across datasets both with and without a background class. Specifically, ViT-B/16 achieves 43.2% mIoU on datasets with a background class, showing a 1.8% mIoU improvement over NACLIP baseline, and 40.3% mIoU on datasets without a background class, with a 2.1% mIoU improvement. These comprehensive results validate that our proposed modules effectively enhance CLIP’s dense prediction capability across various architectures and dataset configurations, demonstrating the robustness and generalization ability of our approach.

C. Extension on other CLIP-like Models

In the main paper, we evaluate our method by integrating it with existing approaches, which are typically improved versions based on the vanilla CLIP model. To further evaluate the effectiveness of our method on other CLIP-like models, we conduct additional experiments on the OpenCLIP [11]. For a fair comparison, we first reproduce the results of SCLIP [46], ClearCLIP [28], and NACLIP [19] on OpenCLIP [11]. Then, we implement the proposed method based on the OpenCLIP [11]. As shown in Table. A2, we present the comprehensive results on datasets without a background class. We can observe that our method shows consistent improvements over different baseline approaches, demonstrating its effectiveness.

Specifically, when integrating SCLIP [46] with our method, ResCLIP achieves significant gains across all datasets, improving the average performance by 1.6% mIoU. The improvement is particularly pronounced on VOC20, where ResCLIP enhances the mIoU from 66.6% to 71.8%. Most notably, integrating ResCLIP with NACLIP [19] yields substantial improvements across all datasets, with an impressive average gain of 2.6% mIoU,

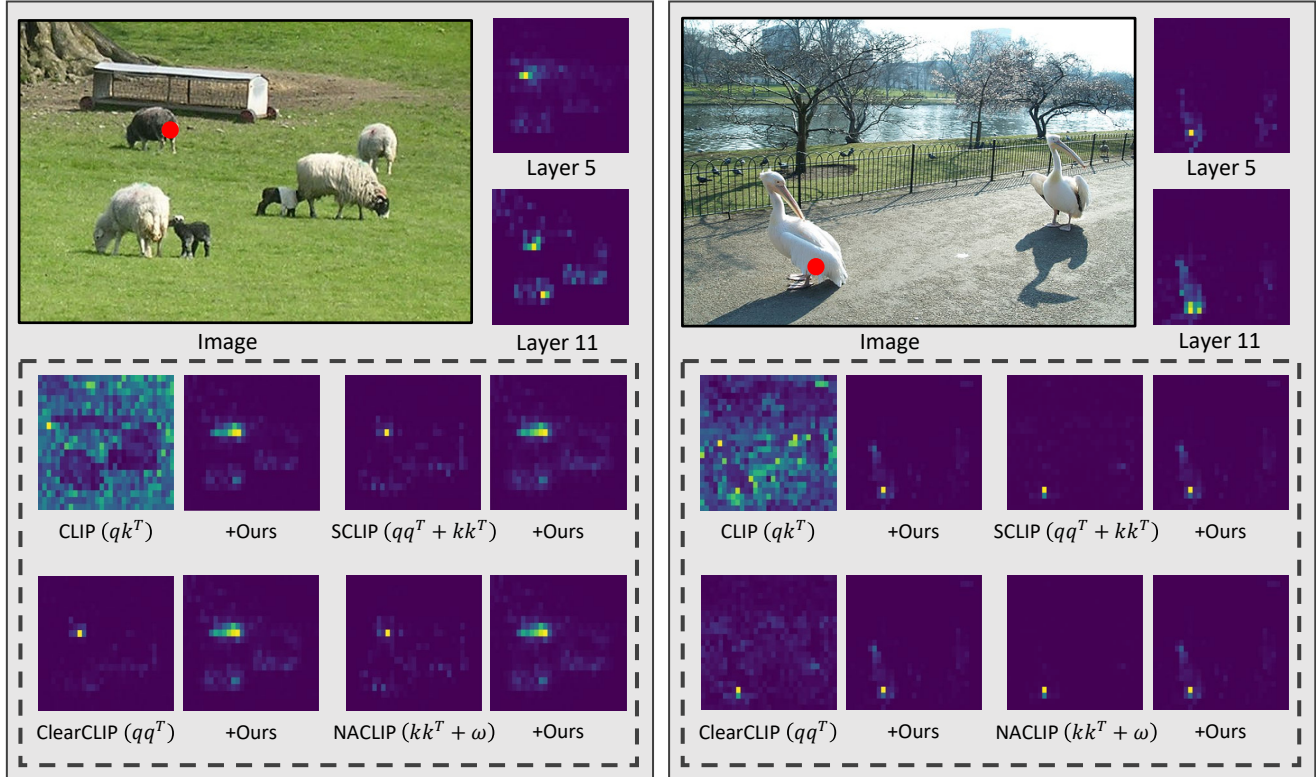


Figure A1. Additional comparison of attention maps across CLIP [38], SCLP [46], ClearCLIP [28], NAACLIP [19], and ours. The attention maps of non-last layers show the localization properties and can heal the attention in the last layer. The red point serves as the source point from which the attention map is computed and visualized.

Table A1. Ablation studies of our proposed modules in ViT-B/16, ViT-B/32 and ViT-L/14 backbones. Our ResCLIP setting is marked in gray. The best result on each dataset is **bolded**. The $\text{Avg}_{w/o}$ means the average mIoU for datasets *without* a background class, $\text{Avg}_{w/}$ means the average mIoU for datasets *with* a background class, and Avg. means the average mIoU for all eight datasets.

Methods	Module		ViT-B/16			ViT-B/32			ViT-L/14		
	<i>RCS</i>	<i>SFR</i>	$\text{Avg}_{w/o}$	$\text{Avg}_{w/}$	Avg.	$\text{Avg}_{w/o}$	$\text{Avg}_{w/}$	Avg.	$\text{Avg}_{w/o}$	$\text{Avg}_{w/}$	Avg.
SCLIP [46]	-	-	37.1	40.0	38.2	32.1	36.2	33.6	23.6	30.5	26.2
+ResCLIP(Ours)	✓	-	38.8	42.4	40.2	34.6	36.9	35.4	36.6	36.9	36.7
	-	✓	37.9	42.0	39.4	32.2	36.4	33.8	28.9	30.5	29.5
	✓	✓	39.3	42.7	40.5	34.8	37.1	35.7	36.7	37.4	37.0
ClearCLIP [28]	-	-	37.5	39.1	38.1	34.8	35.6	35.1	34.5	35.5	34.9
+ResCLIP(Ours)	✓	-	39.7	41.6	40.4	35.3	35.7	35.4	38.3	36.7	37.7
	-	✓	39.4	41.7	40.2	35.1	35.8	35.3	37.0	36.2	36.7
	✓	✓	40.0	42.0	40.7	35.5	35.9	35.6	38.4	37.2	37.9
NAACLIP [19]	-	-	38.2	41.4	39.4	34.4	37.0	35.4	36.2	36.9	36.5
+ResCLIP(Ours)	✓	-	39.7	42.2	40.6	35.7	37.3	36.3	38.4	38.2	38.3
	-	✓	39.3	42.9	40.7	35.7	37.4	36.3	37.4	38.4	37.8
	✓	✓	40.3	43.2	41.4	36.2	37.5	36.7	39.1	39.2	39.1

Table A2. Quantitative comparison on datasets *without* a background class based on OpenCLIP [11] with ViT-B/16 architecture. Our results are marked in gray. The best results on each dataset are **bolded**. Results show that our method is also effective on other VLMs.

Methods	VOC20	Context59	Stuff	Cityscape	ADE20k	Avg.
OpenCLIP [11]	47.2	9.0	5.0	5.1	2.9	13.84
SCLIP [46]	66.6	31.7	21.2	31.4	18.5	33.9
+ResCLIP(ours)	71.8	32.9	21.9	31.9	18.8	35.5 (+1.6)
ClearCLIP [28]	81.4	34.1	23.1	31.8	18.9	37.9
+ResCLIP(ours)	83.3	34.3	23.1	32.3	19.1	38.4 (+0.5)
NACLIP [19]	76.2	30.3	20.3	32.3	17.6	35.3
+ResCLIP(ours)	82.5	33.0	22.2	32.9	19.0	37.9 (+2.6)

including a remarkable 6.3% improvement on VOC20 datasets from 76.2% to 82.5%. These consistent improvements across different CLIP models and datasets demonstrate the generalization of our approach. The results also validate that the observation of our proposed method is effective on other CLIP-like models.

D. Additional Visualization Results

We present additional qualitative comparisons across ADE20K [59], COCO Object [8], and PASCAL VOC [17] datasets in Fig. A2, Fig. A3, and Fig. A4 to further demonstrate the effectiveness of our ResCLIP, respectively. Compared to existing methods, our approach usually presents better quality in terms of the semantic segmentation masks. From these qualitative results, we can have the following observations: 1) Our method generates significantly cleaner segmentation masks with reduced noise artifacts. This improvement is particularly evident in complex scenes from ADE20K, where ResCLIP maintains coherent building segmentation without the internal hollows or fragmentations commonly seen in other baselines (*i.e.*, the 1-st *col.* in Fig. A2). The enhanced segmentation quality extends to diverse scenarios, such as the precise delineation of vehicles in parking lots and the clear separation of multiple instances in crowded scenes (*i.e.*, the 2-nd and 4-th *col.* in Fig. A2). 2) ResCLIP presents superior performance in handling multiple object instances, demonstrating its enhanced spatial-semantic understanding. For example, in the COCO Object dataset (see Fig. A3), our method accurately segments groups of animals while maintaining clear boundaries between individuals (*i.e.*, the 4-th and 5-th *col.* in Fig. A3). This capability stems from the improved attention mechanism of our ResCLIP, which better captures both global spatial relationships and local feature consistency. 3) Our method handles varying scales and perspectives better. As shown in Fig. A4, our method produces consistent segmentation quality across both indoor and outdoor scenes. These qualitative results validate the effectiveness of our proposed RCS and SFR modules in enhancing CLIP’s dense prediction capabilities.

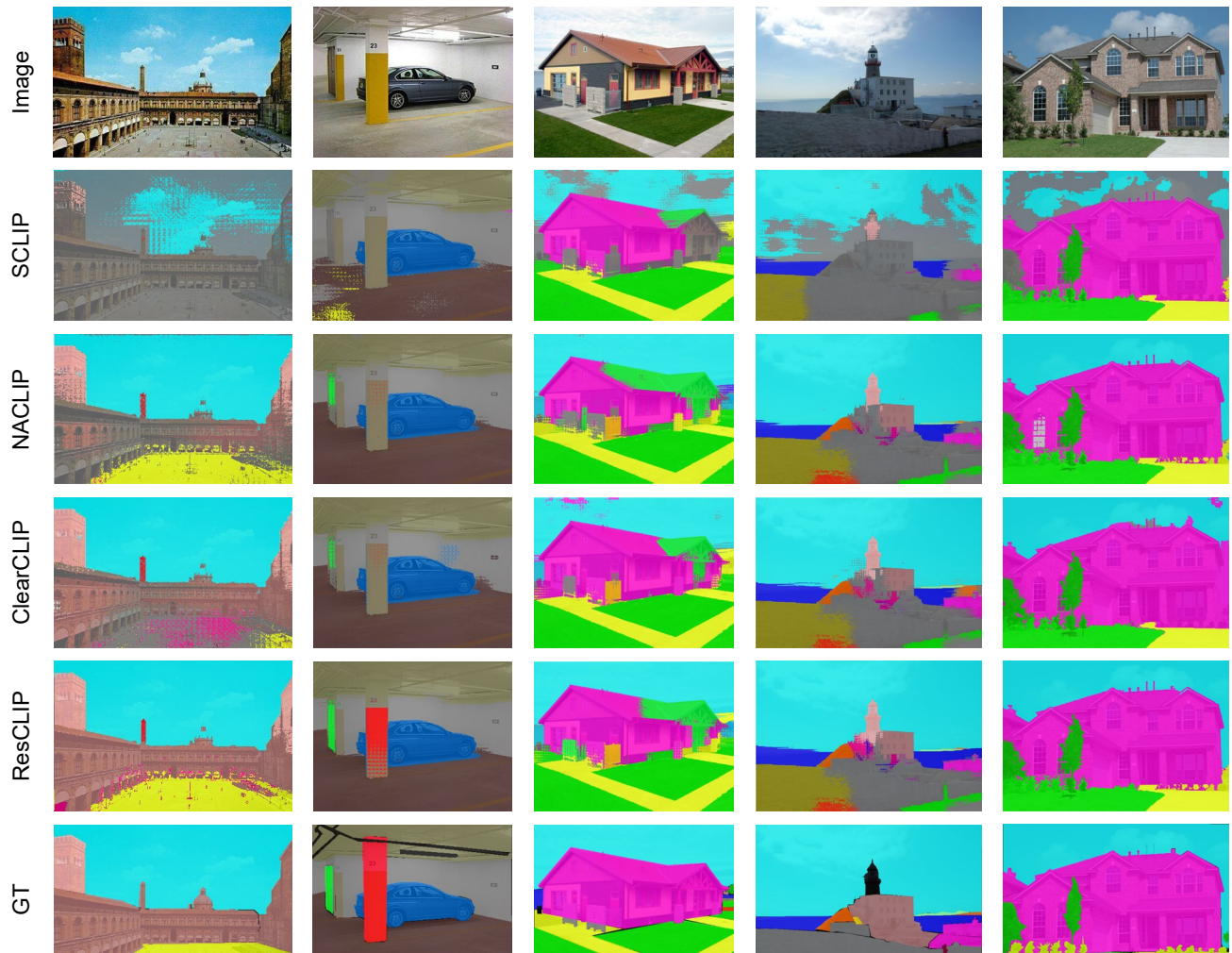


Figure A2. Additional qualitative visualization results among different CLIP-based training-free segmentation methods on ADE20K [59] dataset.



Figure A3. Additional qualitative visualization results among different CLIP-based training-free segmentation methods on COCO Object [8] dataset.

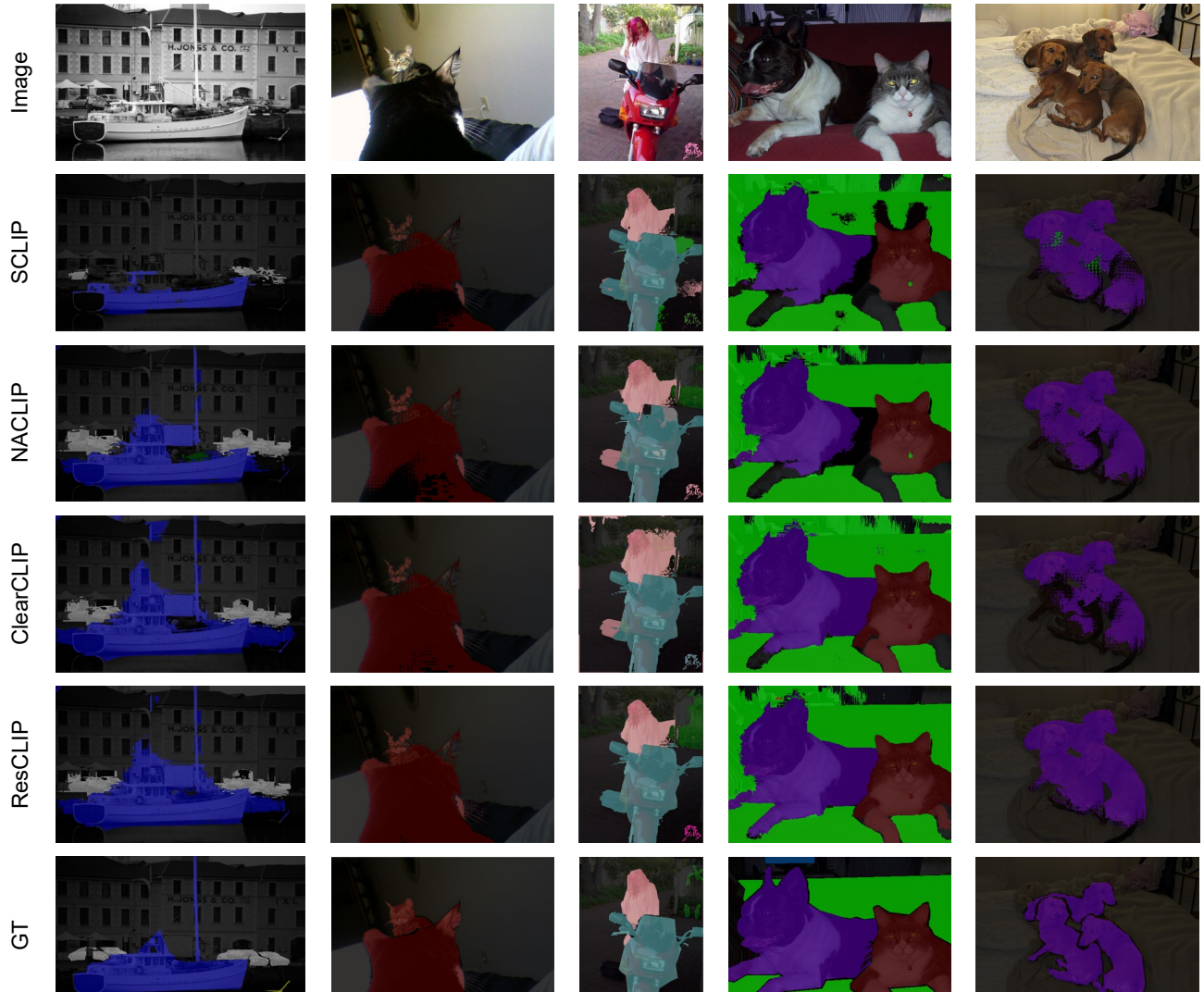


Figure A4. Additional qualitative visualization results among different CLIP-based training-free segmentation methods on PASCAL VOC [17] dataset.